

## Chemical, morphological and structural characterisation of electroless duplex NiP/NiB coatings on steel

Véronique Vitry, Luiza Bonin & Loïc Malet

To cite this article: Véronique Vitry, Luiza Bonin & Loïc Malet (2017): Chemical, morphological and structural characterisation of electroless duplex NiP/NiB coatings on steel, Surface Engineering, DOI: [10.1080/02670844.2017.1320032](https://doi.org/10.1080/02670844.2017.1320032)

To link to this article: <http://dx.doi.org/10.1080/02670844.2017.1320032>



Published online: 26 Apr 2017.



Submit your article to this journal [↗](#)



View related articles [↗](#)



View Crossmark data [↗](#)



## Chemical, morphological and structural characterisation of electroless duplex NiP/NiB coatings on steel

Véronique Vitry <sup>a</sup>, Luiza Bonin<sup>a</sup> and Loïc Malet<sup>b</sup>

<sup>a</sup>Metallurgy Lab, Engineering Faculty, UMONS, Mons, Belgium; <sup>b</sup>4Mat, ULB, Brussels, Belgium

### ABSTRACT

Duplex electroless nickel coatings constituted of one layer of nickel-phosphorous and one of nickel-boron are a promising solution to provide combined wear and corrosion resistance to parts. Duplex systems were compared to systems of similar thickness constituted of only one material, in one or two layers. Duplex coatings present intermediate surface texture, but each layer keeps its typical cross-section morphology and structural features, even after heat treatment. The interfaces between the separate layers are sharp in the as-deposited state but not as much after heat treatment. When nickel-boron is deposited first, it influences slightly the grain growth of the subsequent nickel-phosphorous layer, but no influence can be observed when nickel-phosphorous is deposited first.

### ARTICLE HISTORY

Received 10 January 2017  
Revised 5 April 2017  
Accepted 9 April 2017

### KEYWORDS

Electroless plating; TEM; GDOES; structure; heat treatment; morphology; duplex coatings

### Introduction

The need for increasingly performant materials in industrial applications is a drive for the development of coating technologies that allow increasing the surface properties of materials, like wear and corrosion resistance. Discovered in the late 1940s [1], electroless nickel coatings have been used to this effect for decades [2–5] notably because this method provides coatings with good adherence and near-perfect thickness homogeneity [6–9], due to the catalytic nature of the process that allows plating only the desired surface, without any current repartition effects [2,10,11].

There are two main types of electroless nickel coatings: nickel-phosphorous alloys that are obtained when hypophosphite is used as the reducing agent, with phosphorous content from 2 to 13 wt-% [4,12–16] and nickel-boron alloys that are obtained with either borohydride or amine-borane compounds, whose boron content varies from 0.5 to 9 wt-% [2–4, 7,12,17–21]. Both types of coatings provide relative protection against wear and corrosion, but studies have shown that the corrosion resistance of nickel-phosphorous coatings was better than that of nickel-boron (and that the resistance increased with the phosphorous content), while nickel-boron presented better wear resistance, adhesion and hardness [2,3,12,14]. Moreover, hardness of nickel-phosphorous coatings decreases with P content [2,7,22,23].

There are distinct reports on the use of both types of nickel to improve the properties of similar parts, like for example firearms [4,24–27], one being used for corrosion resistance and the other for wear resistance. The

idea of combining both kinds of coatings to hopefully obtain corrosion and wear resistance at the same time has, thus, been investigated by a few authors [28–32]. However, most of these studies are strictly limited to investigation of the mechanical (and sometimes corrosion) properties of the obtained duplex systems and there is very little information on the morphological and structural effects of using duplex electroless coatings, and even less in the case of heat-treated duplex coatings.

In this paper, the morphology, chemistry and structure of electroless systems, constituted of either one of two layers of nickel-phosphorous and/or nickel-boron will be investigated.

### Experimental details

#### Sample preparation and electroless plating

The substrate chosen for this study was mild steel (ST37-DIN 17100) with a carbon content of 0.17 wt-% and no other major alloying element. Mild steel was chosen because those alloys can be used in numerous applications and because their low alloying element content and rather simple microstructure make them easy to plate by the electroless process.

One mm thickness in coupons of 100 mm × 100 mm was cut from St 37 steel sheets. Holes with a diameter of 2 mm were drilled to allow handling of the samples.

Before electroless plating, the samples were ground with SiC abrasive paper up to a grit of 2000. They were then degreased with acetone and etched in 30 vol.-% HCl just before plating.

**Table 1.** Operating conditions for electroless nickel-boron plating.

NiB		NiP	
NiCl <sub>2</sub> ·6H <sub>2</sub> O	24 g L <sup>-1</sup>	Niklad ELV 808A and Niklad ELV 808B, according to user manual	
NaOH	39 g L <sup>-1</sup>		
Ethylenediamine	60 mL L <sup>-1</sup>		
PbWO <sub>4</sub>	0.021 g L <sup>-1</sup>		
NaBH <sub>4</sub>	0.602 g L <sup>-1</sup>		
Bath temperature	96.5 ± 0.5°C	Bath temperature	88 ± 1°C
Bath pH	13.5	Bath pH	5.75
Plating time		Plating time	
for 10 µm	32 min	for 10 µm	35 min
for 20 µm	70 min	for 20 µm	70 min

Two types of electroless nickel coatings were used in this study: a mid-phosphorous commercial solution (Niklad ELV 808A and Niklad ELV 808B from Mc Dermid with a typical content of 7–9 wt-% P) was used for the nickel-phosphorous coating. A nickel-boron plating bath developed at UMONS [33], which contains nickel chloride, sodium borohydride, ethylene diamine and lead tungstate, was used for the nickel-boron plating. Plating conditions for the nickel-boron bath were slightly modified to increase the boron content of the coating [32]. The composition and plating conditions for both plating baths can be found in Table 1.

Several types of samples were produced in this study: monolayer electroless nickel samples (both NiP and NiB) with a thickness of 20 µm, bilayer samples composed of two layers of the same electroless nickel composition and a total thickness of 20 µm and duplex samples combining 10 µm of nickel-boron and 10 µm of nickel-phosphorous. The bilayer samples were not made with applications in mind but to observe if the presence of a homogeneous interface (where the same material is present on both sides of the interface) modified the properties of the coating.

To ensure repeatability of the plating process, an 8 L bath was used for the thinner coatings (10 µm) and a 10 L bath for the 20 µm layers. Plating rate was repeatedly measured to determine the exact plating time needed to plate 10 and 20 µm of each coating.

For bilayer and duplex systems, a new bath was used for each layer and the samples were rinsed, dried and stored in a desiccator after the deposition of the first layer. The time lapse between successive plating processes was kept as short as possible (always lesser

than 6 h), to avoid degradation of the surface activity of the previously deposited layer. A summary of the types of coatings synthesised for this study can be found in Figure 1.

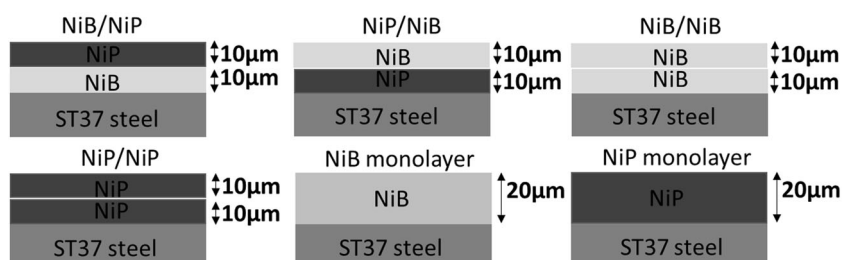
To assess the effect of heat treatment on the coatings, some samples were submitted to a treatment carried out at 400°C for 1 h under a slightly reducing atmosphere (95% Ar and 5% H<sub>2</sub>) to avoid alterations of the surface properties. The heating rate was 50° C min<sup>-1</sup> and the samples were cooled in the turned off furnace, still under reducing atmosphere. This heat treatment was selected because it is popular for both NiP [16,34–35,23] and NiB [8,21,36,37] coatings and has moreover proved to be effective for the nickel boron coating used in this study [38].

### Characterisation methods

The depth-profile chemistry of the samples was investigated by GDOES analysis using a calibrated Horiba-Jobin-Yvon GD-Profilier 2. Average composition of the different layers was derived from the GDOES analysis. The surface aspect of samples was observed with a Hirox 8700 3D optical microscope. Cross-sections were mounted and prepared for metallographic analysis by polishing up to a mirror finish and etching for 180 s with 10 vol.-% nital. They were observed by SEM using a JEOL JSM 5900 LV electron microscope.

Structural analysis of the samples was carried out by X-ray diffraction with the use of a Siemens D50 spectrometer in  $\theta$ -2 $\theta$  configuration and using Cobalt K $\alpha$  radiation (1.79 Å). Diffraction peaks were indexed using the 'Match' software (Crystal Impact, Match! – Phase Identification from Powder Diffraction – version 1.11).

TEM observations of selected samples were carried out using a Philips CM 20 electron microscope, operating at 200 kV. The thin sections of selected samples were prepared by focused ion-beam machining in a FEI Quanta 200 3D dual beam apparatus. Sections were cut parallel to the growth direction of the coating by the selected area lift out method on polished cross-sections of the samples. The aim was to complete the morphological and structural characterisation of the monolayers and to observe the interface between the two electroless nickel layers in duplex coatings.

**Figure 1.** Summary of the various coating systems.

## Results and discussion

### Chemical analysis of the coatings

GDOES depth-profile analysis results for all samples are shown in Figures 2 and 3 as well as in Table 2. The boron content of all coatings seems to not have been affected by the plating conditions, as average values are always close to 6.8%, with lead contents close to 1.4 wt-%. The results indicate that the modification of plating conditions allowed increasing the boron content from 4.5 to 5.5 wt-% [39] to nearly 7 wt-% without modifying the lead content in an unacceptable manner.

However, it appears that using a lower bath load (a bigger bath for a sample of the same dimensions) to obtain a thicker coating leads to a decrease in the phosphorous content, as can be seen in Table 2 and Figure 1(a). However, the P content obtained in all cases stays in the limits of the industrial bath information: 7–9 wt-% P.

Careful examination of the depth profiles shows that the boron content of the nickel-boron coatings tends to

be similar at the beginning and the end of the plating process with a decrease in the boron content in the top 1–2  $\mu\text{m}$  (Figure 2(b,c,f)). The lead content follows similar trends to those of the boron content in all samples. It appears that using a lower bath load also modifies the chemistry of the boron coatings but in a more local manner: samples used with higher loads present higher variations of boron (Figure 2(d,e,f)) content in the coating, similarly samples obtained at lower temperature using the same bath load [40] while those obtained at lower loads present a more homogeneous chemistry.

The variations of phosphorous content are very different from those of boron, with an overall continuous increase of phosphorous during the plating process (Figure 2(a,c,e)).

The interface between successive phosphorous layers is clearly observable due to the sharp modification of phosphorous content linked with the use of a new bath (Figure 2(c)). However, in the case of nickel-boron coatings, there is no such variation to be observed or they are masked by the roughness of

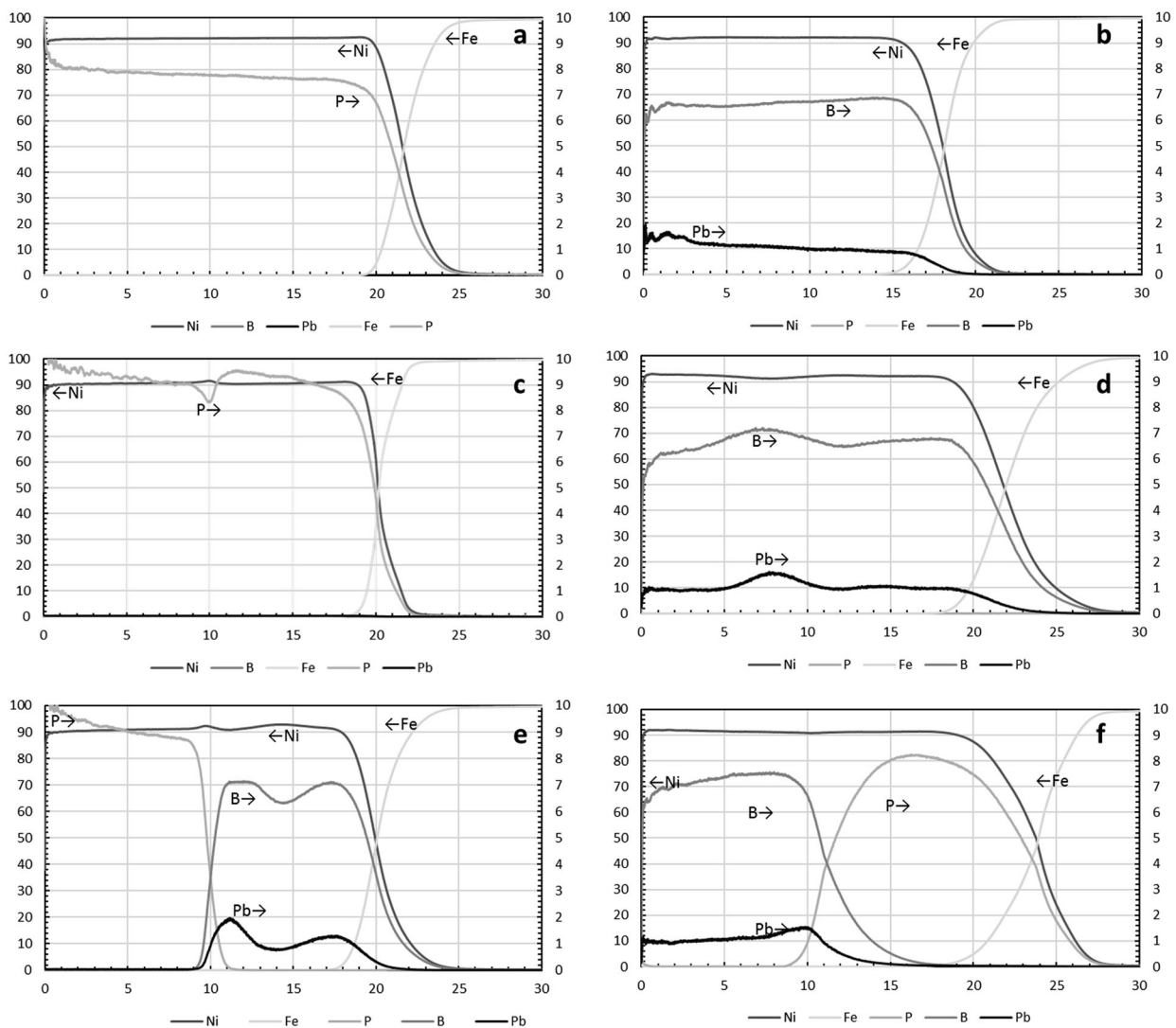


**Figure 2.** GDOES depth-profile analysis of as-plated electroless nickel coatings: (a) NiP monolayer; (b) NiB monolayer; (c) NiP bilayer; (d) NiB bilayer; (e) steel/NiB/NiP duplex; (f) steel/NiP/NiB duplex.

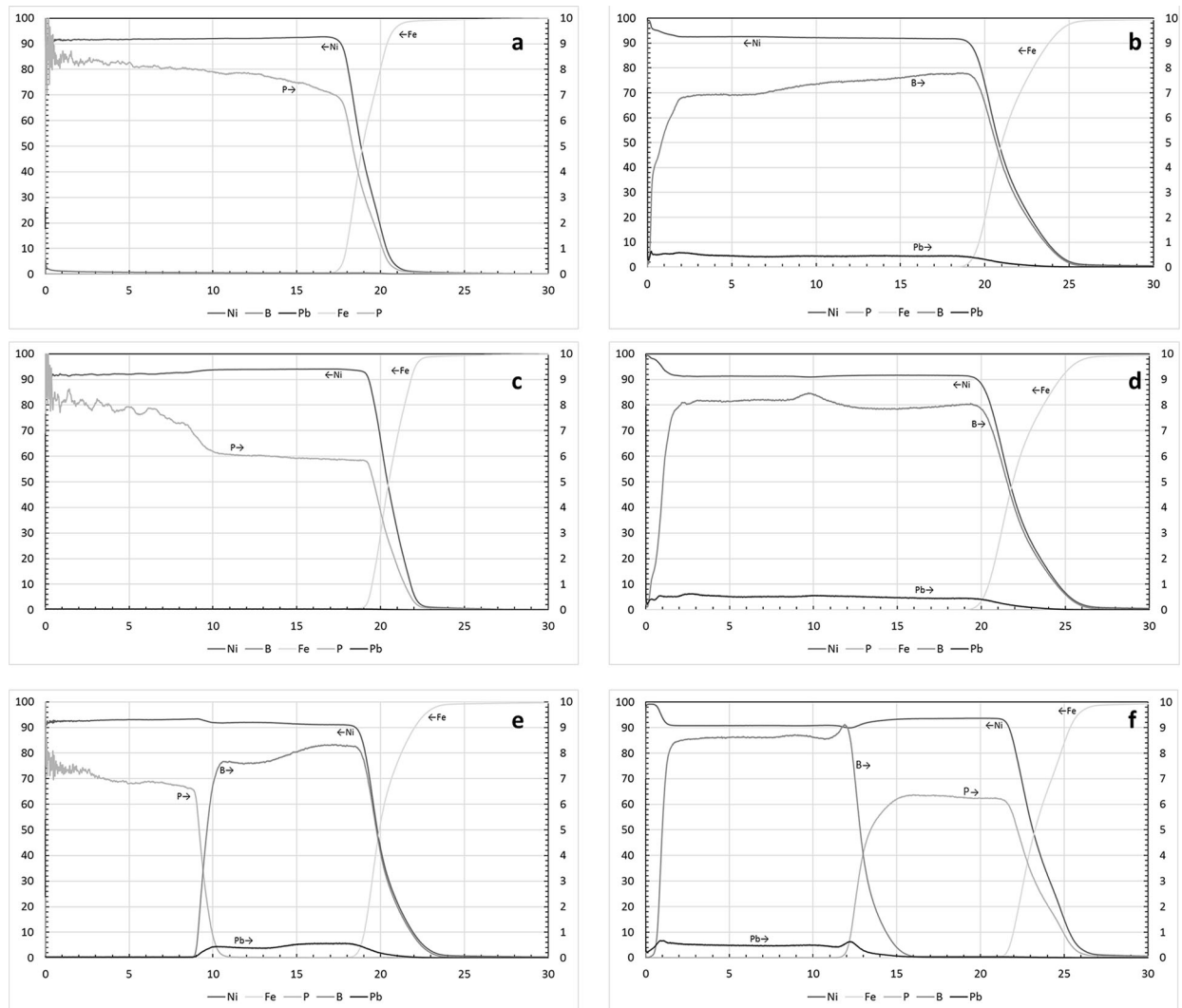


**Figure 3.** GDOES depth-profile analysis of heat-treated electroless nickel coatings: (a) NiP monolayer; (b) NiB monolayer; (c) NiP bilayer; (d) NiB bilayer; (e) steel/NiB/NiP duplex; (f) steel/NiP/NiB duplex.

the interface between the two nickel-boron layers (Figure 2(d)).

Heat treatment has no effect on average composition of the coatings but can lead to significant local variations of concentration, as can be seen in Figure 3. In the case of nickel-phosphorous, heat treatment leads to an increase in P content close to the sample surface (Figure 3(a,c,e)) which suggests that some of the phosphorous may diffuse to form compounds on the surface of the coating during the heat treatment. Diffusion is also observed at the substrate/coating interface in all samples, but in a rather limited manner, as attested by the rather sharp

decrease in iron and increase in nickel at the interface. Boron, once again, has a different behaviour: it diffuses rather towards the inside of the sample, which leads to higher boron content at the interface with the substrate or the underlying layer (Figure 3 (b,d,e,f)) and to low boron contents at the free surface of the sample. It is thus expected that the crystalline structure of the nickel-boron layer may vary from the interface to the free surface. Lead once again follows the evolution of the boron content in all the nickel-boron coatings.

### Coating morphology

The surface morphology of mono- and bilayer coatings corresponds to the usual surface aspect of the type of coating deposited on the substrate: nickel-boron presents the typical cauliflower-like surface texture [2,19,41] (see Figure 4(a,b)), while nickel-phosphorous presents a planar morphology also usual for this type of coating (Figure 4(d,e)) [2,42,43]. Duplex coatings present intermediate

**Table 2.** Average composition of electroless nickel coatings.

(wt-%)	Ni	P	B	Pb
Duplex Ni-B/Ni-P	91.39	9.14	6.72	1.21
Duplex Ni-P/Ni-B	90.01	7.79	7.18	1.47
Bilayer NiB	92.13		6.66	1.07
Monolayer Ni-B	91.99		6.66	1.11
Bilayer Ni-P	90.65	9.20		
Monolayer Ni-P	92.06	7.78		

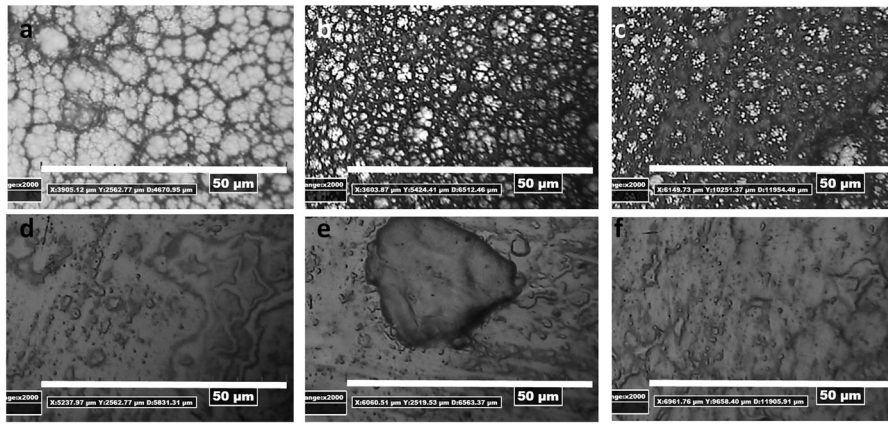


**Figure 4.** Surface morphology of electroless Ni-P/Ni-B duplex, monolayer and bilayer coatings – as-plated conditions.

features but are more influenced by the top layer: when boron is the upper layer, and slightly attenuated cauliflower-like texture can be observed (Figure 4(c)), while the duplex coating with nickel-phosphorous on top (Figure 4(f)) does present very attenuated features, showing the very good dimensional conservation of the nickel-phosphorous coating.

As can be seen in Figure 5, heat treatment does not modify the surface texture of the samples.

Cross-section of the samples was observed by SEM after etching and is presented in Figure 6. Nickel-phosphorous appears featureless on those images (it is not etched by nital), as can be seen in Figure 6(c,d,e,f). It is not even possible to observe the separation of the two NiP layers in the bilayer coating (Figure 6(e)). Nickel-boron presents a columnar morphology typical for those coatings (Figure 6(a,b,c,f)) [2,24,40,44] and the delimitation between the two successive layers (Figure 6(b)) can be very easily observed and looks similar to the effect of batch bath replenishment [45]. In the case of duplex coatings (Figure 6(c,f)), the two layers are clearly delimited and keep their typical features. However, the interface obtained when nickel-phosphorous constitutes the first layer (Figure 6(c)) is totally planar, while that obtained when nickel-boron is deposited first is slightly wavy due to the columnar growth in that coating.

Heat treatment does not modify the morphology of the coatings, as can be deduced from the comparison of the left (as plated) and right (heat treated) parts of Figure 6.

### Coatings structure observed by XRD

X-ray diffraction results are shown in Figure 7 for as-plated coatings and Figure 8 for heat-treated samples. In the as-plated state (Figure 7), all the coatings present a broad peak centred around  $53^\circ$  that indicates the presence of amorphous or nanocrystalline supersaturated nickel. Coatings where nickel-phosphorous constitutes the top layer (i.e. NiP mono- and bilayer and Steel/NiB/NiP duplex coating) present slightly sharper peaks, which suggests that nickel-phosphorous is more crystallised or presents bigger grain sizes than nickel-boron.

After heat treatment (Figure 8), two nickel peaks (at  $52^\circ$  and  $61^\circ$ ) are observed for all samples. Only the top 10  $\mu\text{m}$  of the sample can be analysed by this method, so the bottom layer of duplex coatings is not observed. When nickel-boron constitutes the top layer, nickel and two boride phases are observed:  $\text{Ni}_3\text{B}$  and  $\text{Ni}_2\text{B}$ . Their presence is consistent with the chemistry of the coating:  $\text{Ni}_3\text{B}$  corresponds to a boron content of 5.8 wt-%. It is thus expected that a smaller but non-negligible amount of  $\text{Ni}_2\text{B}$  (that corresponds to 8.5 wt-%B)

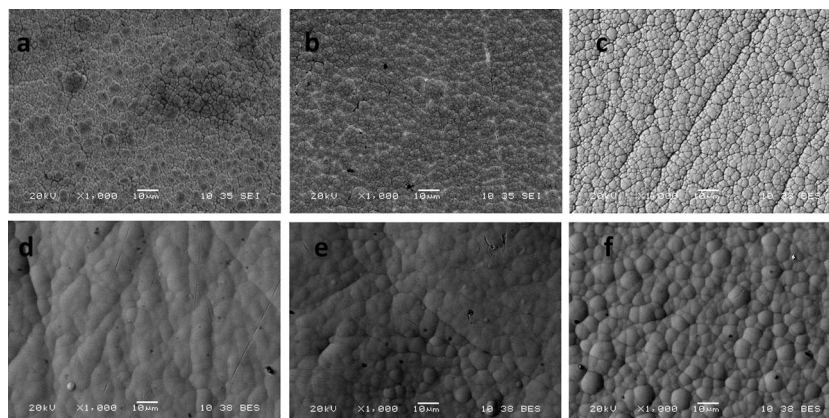


**Figure 5.** Surface morphology of electroless Ni-P/Ni-B duplex, monolayer and bilayer coatings – heat treated.

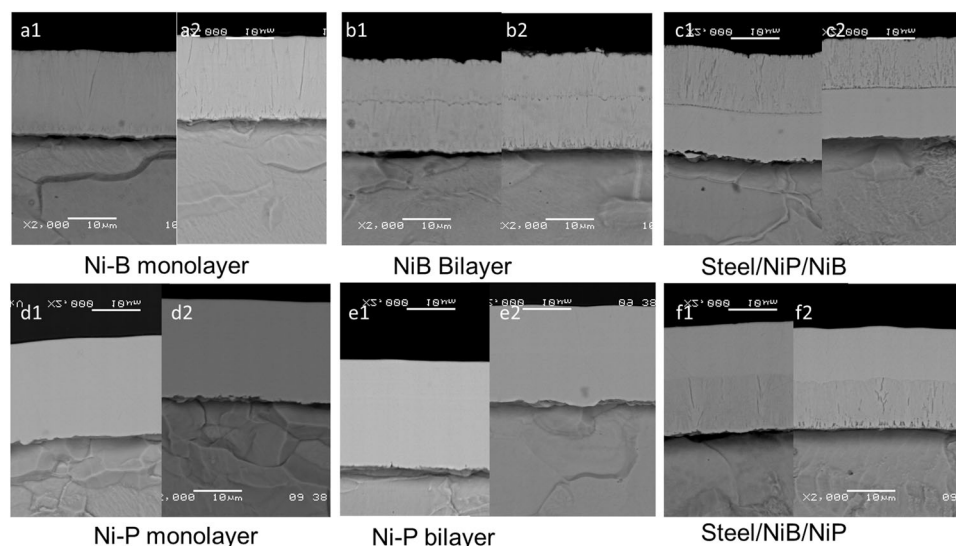


**Figure 6.** Cross-section morphologies of electroless Ni-P/Ni-B duplex, monolayer and bilayer coatings (a) NiB monolayer; (b) NiB bilayer; (c) steel/NiP/NiB; (d) NiP monolayer; (e) NiP bilayer; (f) steel/ NiB/NiP. Left side (1) as plated; right side (2) heat treated.

is formed during the heat treatment. This is amplified by the diffusion phenomena observed during the heat treatment, leading to the formation of a nickel-enriched zone which is the origin of the appearance of a metallic nickel peak. When nickel-phosphorous is the top layer, only  $\text{Ni}_3\text{P}$  (15 wt-% P) and nickel can be observed, which is consistent with the chemistry of the coatings.

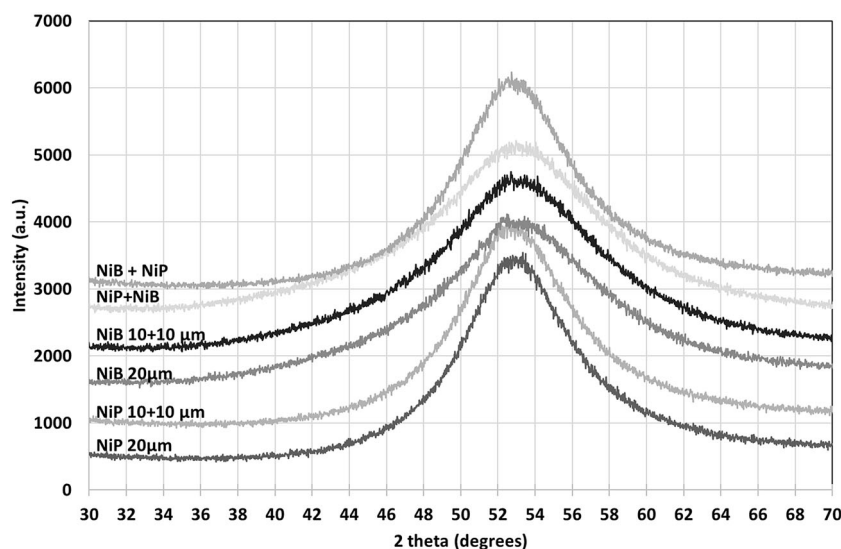
### TEM observation of the coatings and interfaces

Figure 9 presents the lifted-out sample obtained from a steel/NiP/NiB duplex coating. All interfaces are clearly identifiable, which will allow us to target the observation zones.

The microstructure and electron diffraction pattern of the NiP monolayer coating are presented in Figure 10. In the as-deposited state, NiP presents a nanocrystalline structure, in accordance with the chemistry of the

coating and the XRD results. The selected area electron diffraction (SAED) pattern (Figure 10(c)) is constituted of several distinct and slightly fuzzy rings, which indicates that the grain size is very small. This is confirmed by the TEM brightfield image (Figure 10(a)), where grains with a size close to 10 nm can be observed. After heat treatment, the diffraction pattern (Figure 10 (d)) indicates complete crystallisation with several grains in the selected area. The crystalline phase is  $\text{Ni}_3\text{P}$  as expected from chemistry and XRD (the image was voluntarily non-indexed to keep maximal legibility). This is confirmed by the TEM image, where grains with a size close to 30–50 nm are observed.

In the as-deposited state, monolayer NiB presents a nearly amorphous state, as attested by the presence of only one well-defined ring in the SAED pattern (Figure 11 (c)). However, the presence of a hazy second ring suggests that short distance order is conserved, similarly to what



**Figure 7.** X-ray diffraction results for as-plated electroless nickel coatings.

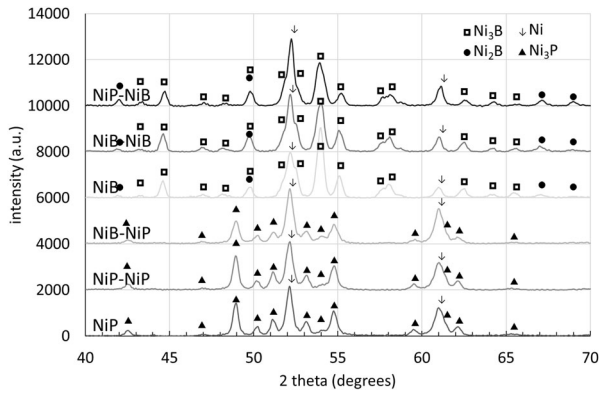


**Figure 8.** X-ray diffraction results for heat-treated electroless nickel coatings.

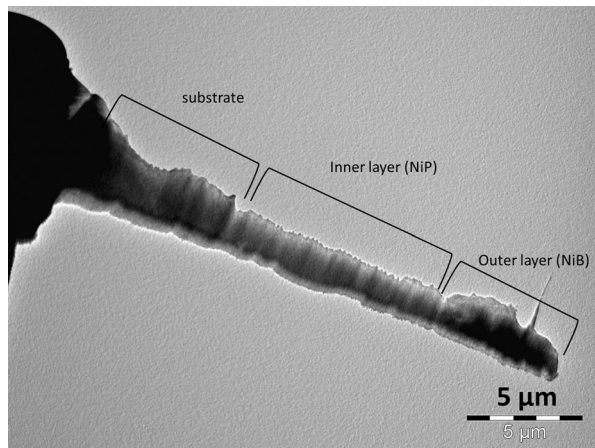


**Figure 9.** TEM image of a thin section of a duplex electroless nickel-coating.

was observed for coatings with a lower boron content [39]. The grain size cannot be measured on the TEM image, but a wavy pattern, similar in shape to the top of the columnar texture of the coating, can be observed in the sample (Figure 11(a)). Those were already observed in other nickel-boron deposits [39] and suggest a layer-by-layer growth of the coating. After heat treatment, the structure and morphology of the coating differs according to the position: near the substrate and in the bulk, big anisotropic  $Ni_3B$  grains (100 nm or more, Figure 11(b)) can be observed. However, much smaller Ni grains (10 nm) are observed in the superficial zone (Figure 11(d)), in accordance with the decrease of boron content near to the surface of the sample.

The TEM observation of monolayer samples confirms thus the findings of XRD and SEM analysis and are fully in accordance with chemical analysis.

The interfaces between electroless nickel-phosphorous and nickel-boron layers are shown in Figure 12. When nickel-phosphorous is deposited first (Figure 12(a,c)), the interface between both layer is clearly delimited and planar and there is no apparent influence of the first layer on the formation of the second one. The features of NiB cannot be observed at the magnification of Figure 12(a). The interface is very clear in the as-deposited state (Figure 12(a)), but it is difficult to judge for heat-treated samples (Figure 12(c)). When nickel-boron constitutes the first layer, the interface is wavy but sharp in the as-deposited state (Figure 12(b)), as expected from SEM observations; however, this does not influence the growth of the nickel-phosphorous layer. After heat treatment (Figure 12(d)), the interface stays wavy but loses some of its sharpness, probably due

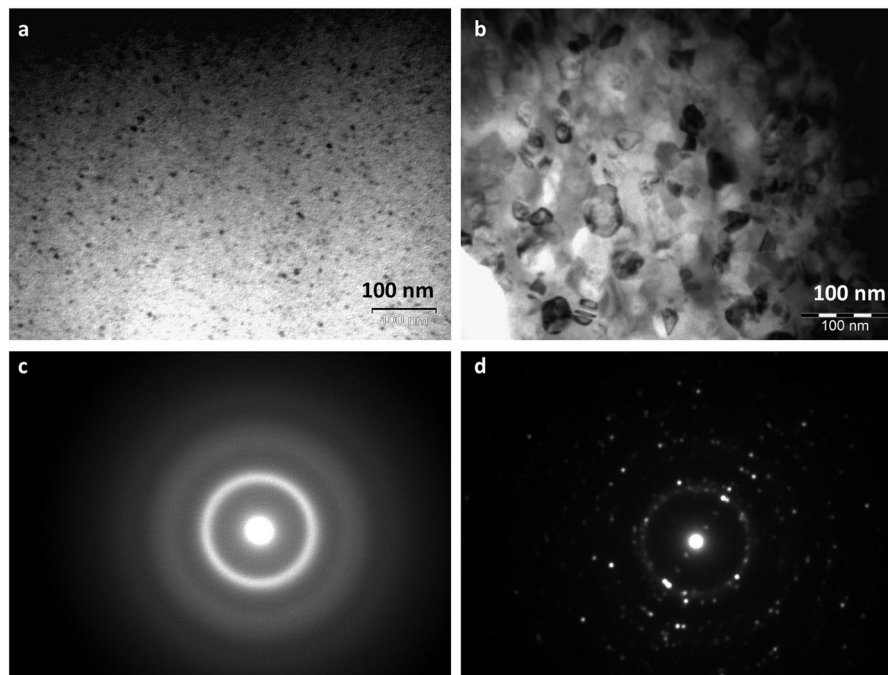


**Figure 10.** TEM characterisation of NiP monolayer coating. (a) Morphology, as deposited; (b) morphology, heat treated; (c) electron diffraction pattern, as deposited; (d) electron diffraction pattern, heat treated.

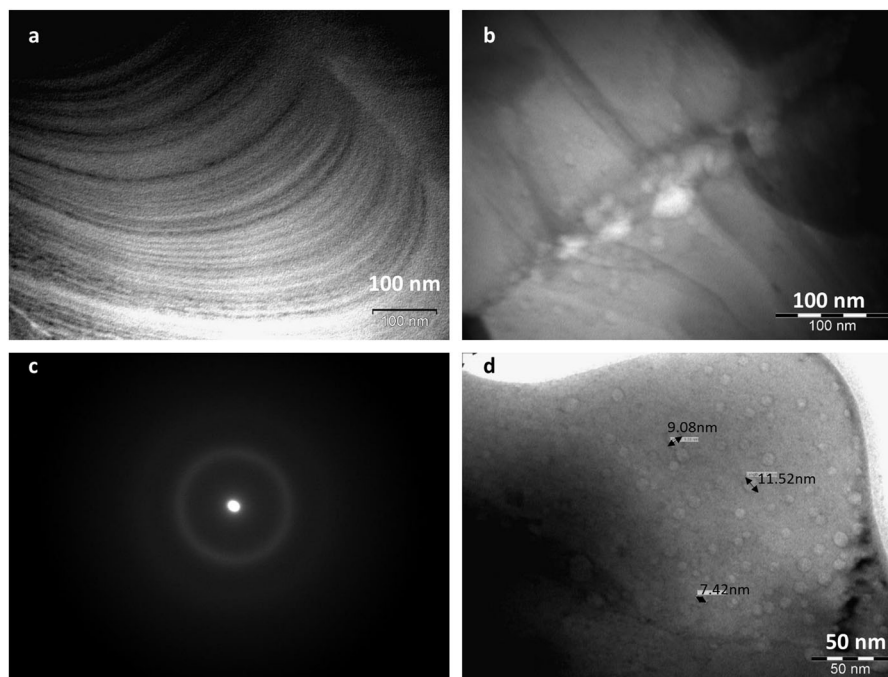


**Figure 11.** TEM characterisation of NiB monolayer coating. (a) Morphology, as deposited; (b) morphology, heat treated: bulk; (c) electron diffraction pattern, as deposited; (d) morphology, heat treated: superficial zone.

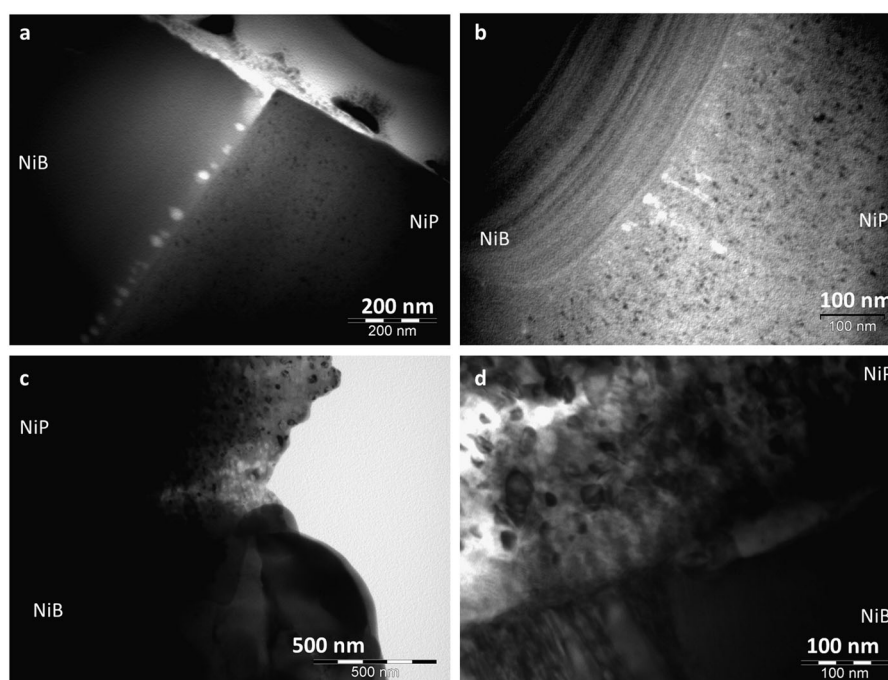


**Figure 12.** TEM characterisation the interface of duplex electroless coatings. (a) NiP/NiB, as deposited; (b) NiB/NiP, as deposited; (c) NiP/NiB, heat treated; (d) NiB/NiP, heat treated.

to interdiffusion. The nickel-phosphorous grains closest to the interface appear elongated rather than isotropic, which may be due to the presence of columnar features in the undelaying nickel-boron.

## Conclusions

Electroless nickel mono, bilayers and duplex coatings have been chemically, morphologically and structurally characterised.

Individual layers present features typical for the type of coating:

- As -deposited nickel-phosphorous is constituted of nanocrystalline supersaturated nickel with isotropic grains whose size is close to 10 nm. They do not present any observable growth feature (neither layered nor columnar).
- After heat treatment, electroless NiP crystallises in the Ni<sub>3</sub>P form, with isotropic grains in the

30–50 nm range and no observable microscale features.

- NiB coatings present a nearly amorphous structure in the as-deposited state and their growth pattern can be observed by SEM (columnar/feather-like morphology) and by TEM, wavy-layered features.
- After heat treatment, due to local modifications of the chemistry of the coating, nickel-boron presents big (>100 nm) Ni<sub>3</sub>B grains close to the interface and much smaller Ni grains close to the surface. The big Ni<sub>3</sub>B grains are slightly anisotropic, thus conserving the columnar features observed by SEM.
- The interfaces between NiP and NiB are very sharp in the as-deposited state and less clearly defined after heat treatment. When NiP has been deposited first, the interface is completely planar, in accordance with the superficial features of the coating. When NiB is the first deposited layer, wavy interfaces are observed.
- No influence of the first layer on the growth of the second one has been identified, but the nickel-phosphorous grains closest to the interface, when nickel-boron is the first layer, present slight anisotropy.

## Acknowledgements

The authors thank the Materia Nova Research Center for technical support in the use of SEM. They also thank Mr Didier Robert for his help with FIB milling of the samples.

## Disclosure statement

No potential conflict of interest was reported by the authors.

## Funding

One of the authors thanks the CNPq (Conselho Nacional de Desenvolvimento Científico e Tecnológico) for funding.

## ORCID

Véronique Vitry  <http://orcid.org/0000-0002-9155-7271>

## References

- [1] Brenner, A, Riddell, GE. Nickel plating on steel by chemical reduction; 1946.
- [2] Riedel, W. Electroless nickel plating. London: Finishing Publication LTD; 1989.
- [3] Sudagar J, Lian J, Sha W. Electroless nickel, alloy, composite and nano coatings – a critical review. *J Alloys Compd.* 2013;571:183–204.
- [4] Agarwala RC, Agarwala V. Electroless alloy/composite coatings: a review. *Sadhana.* 2003;28:475–493.
- [5] Gawne DT, Ma U. Engineering properties of chromium plating and electroless and electroplated nickel. *Surf Eng.* 1988;4:239–249.
- [6] Vitry V, Delaunois F, Dumortier C. Mechanical properties and scratch test resistance of nickel-boron coated aluminium alloy after heat treatments. *Surf Coatings Technol.* 2008;202:3316–3324.
- [7] Sahoo P, Das SK. Tribology of electroless nickel coatings – a review. *Mater Des.* 2011;32:1760–1775.
- [8] Delaunois F, Lienard P. Heat treatments for electroless nickel-boron plating on aluminium alloys. *Surf Coatings Technol.* 2002;160:239–248.
- [9] Krishnan KH, John S, Srinivasan KN, et al. An overall aspect of electroless Ni-P depositions – a review article. *Metall Mater Trans.* 2006;37:1917–1926.
- [10] Abrantes LM, Correia JP. On the mechanism of electroless Ni-P plating. *J Electrochem Soc.* 1994;141:2356.
- [11] Wang TC, Chen B, Rubner MF, et al. Selective electroless nickel plating on polyelectrolyte multilayer platforms. *Langmuir.* 2001;17:6610–6615.
- [12] Vitry, V, Delaunois, F. Electroless nickel-phosphorous vs electroless nickel-boron: comparison of hardness, abrasion resistance, scratch test response and corrosion behavior. In: Aliofkhaezrai, M, editor. *Comprehensive guide for nanocoatings technology, volume 1: deposition and mechanism.* Nova Science Publishers; 2015. p. 145–173.
- [13] Jiaqiang G, Yating W, Lei L, et al. Crystallization temperature of amorphous electroless nickel-phosphorus alloys. *Mater Lett.* 2005;59:1665–1669.
- [14] Vitry V, Sens A, Delaunois F. Comparison of various electroless nickel coatings on steel: structure, hardness and abrasion resistance. *Mater Sci Forum.* 2014;783–786:1405–1413.
- [15] Choudhury BS, Sen RS, Oraon B, et al. Statistical study of nickel and phosphorus contents in electroless Ni-P coatings. *Surf Eng.* 2009;25:410–414.
- [16] Rahimi AR, Modarres H, Abdouss M. Study on morphology and corrosion resistance of electroless Ni-P coatings. *Surf Eng.* 2009;25:367–371.
- [17] Shakoor RA, Kahraman R, Gao W, et al. Synthesis, characterization and applications of electroless Ni-B coatings – a review. *Int J Electrochem Sci.* 2016;11:2486–2512.
- [18] Wang ZC, Jia F, Yu L, et al. Direct electroless nickel-boron plating on AZ91D magnesium alloy. *Surf Coatings Technol.* 2012;206:3676–3685.
- [19] Correa E, Zuleta AA, Sepúlveda M, et al. Nickel-boron plating on magnesium and AZ91D alloy by a chromium-free electroless process. *Surf Coatings Technol.* 2012;206:3088–3093.
- [20] Madah F, Dehghanian C, Amadeh AA. Investigations on the wear mechanisms of electroless Ni-B coating during dry sliding and endurance life of the worn surfaces. *Surf Coatings Technol.* 2015;282:6–15.
- [21] Srinivasan KN, Meenakshi R, Santhi A, et al. Studies on development of electroless Ni-B bath for corrosion resistance and wear resistance applications. *Surf Eng.* 2010;26:153–158.
- [22] Ambat R, Zhou W. Electroless nickel-plating on AZ91D magnesium alloy: effect of substrate microstructure and plating parameters. *Surf Coatings Technol.* 2004;179:124–134.
- [23] Keong K, Sha W, Malinov S. Hardness evolution of electroless nickel-phosphorus deposits with thermal processing. *Surf Coatings Technol.* 2003;168:263–274.
- [24] Riddle, YW, Bailer, TO. Friction and wear reduction via an {Ni-B} electroless bath coating for metal alloys. *JOM.* April 2005;57:40–45.
- [25] Vermot, S. Timepiece escapement lever, US Patent US3738101 A; 1972.
- [26] Brown, J. Non-toxic shot, US patent US4714023 A; 1986.

- [27] McComas, E. Nodular nickel boron coating, US patent US6782650 B2; 2002.
- [28] Narayanan TSNS, Krishnaveni K, Seshadri SK. Electroless Ni-P/Ni-B duplex coatings: preparation and evaluation of microhardness, wear and corrosion resistance. *Mater Chem Phys.* 2003;82:771–779.
- [29] Vitry V, Sens A, Kanta AF, et al. Wear and corrosion resistance of heat treated and as-plated duplex NiP/NiB coatings on 2024 aluminum alloys. *Surf Coatings Technol.* 2012;206:3421–3427.
- [30] Zhang WXX, Jiang ZHH, Li GYY, et al. Electroless Ni-P/Ni-B duplex coatings for improving the hardness and the corrosion resistance of AZ91D magnesium alloy. *Appl Surf Sci.* 2008;254:4949–4955.
- [31] Tohidi A, Monirvaghefi SM, Hadipour A. Properties of electroless Ni-B and Ni-P/Ni-B coatings formed on stainless steel. *Trans Indian Inst Met.* 2016: 1–8.
- [32] Bonin L, Vitry V. Mechanical and wear characterization of electroless nickel mono and bilayers and high boron-mid phosphorous electroless nickel duplex coatings. *Surf Coatings Technol.* 2016;307:957–962.
- [33] Delaunois F, Petitjean JP, Jacob-Dulière M, et al. Autocatalytic electroless nickel-boron plating on light alloys. *Surf Coatings Technol.* 2000;124:201–209.
- [34] Keong KG, Sha W. Crystallisation and phase transformation behaviour of electroless nickel-phosphorus deposits and their engineering properties. *Surf Eng.* 2002;18:329–343.
- [35] Tomlinson WJ, Mayor JP. Formation, microstructure, surface roughness, and porosity of electroless nickel coatings. *Surf Eng.* 1988;4:235–238.
- [36] Vitry V, Kanta AF, Delaunois F. Mechanical and wear characterization of electroless nickel-boron coatings. *Surf Coatings Technol.* 2011;206:1879–1885.
- [37] Pal S, Verma N, Jayaram V, et al. Characterization of phase transformation behaviour and microstructural development of electroless Ni-B coating. *Mater Sci Eng A.* 2011;528:8269–8276.
- [38] Vitry V, Bonin L. Increase of boron content in electroless nickel-boron coating by modification of plating conditions. *Surf Coatings Technol.* 2017;311:164–171.
- [39] Vitry V, Kanta AF, Dille J, et al. Structural state of electroless nickel-boron deposits (5wt.% B): characterization by XRD and TEM. *Surf Coatings Technol.* 2012;206:3444–3449.
- [40] Vitry V, Sens A, Kanta AF, et al. Experimental study on the formation and growth of electroless nickel-boron coatings from borohydride-reduced bath on mild steel. *Appl Surf Sci.* 2012;263:640–647.
- [41] Anik M, Körpe E, Şen E, et al. Effect of coating bath composition on the properties of electroless nickel-boron films. *Surf Coatings Technol.* 2008;202:1718–1727.
- [42] Alexis J, Gaussens C, Etcheverry B, et al. Development of nickel-phosphorus coatings containing micro particles of talc phyllosilicates. *Mater Chem Phys.* 2013;137:723–733.
- [43] Sha W, Wu X, Sarililah W. Scanning electron microscopy study of microstructural evolution of electroless nickel-phosphorus deposits with heat treatment. *Mater Sci Eng B Solid-State Mater Adv Technol.* 2010;168:95–99.
- [44] Vitry V, Delaunois F. Formation of borohydride-reduced nickel-boron coatings on various steel substrates. *Appl Surf Sci.* 2015;359:692–703.
- [45] Vitry V, Kanta AF, Delaunois F. Evolution of reactive concentration during borohydride-reduced electroless nickel-boron plating and design of a replenishment procedure. *Ind Eng Chem Res.* 2012;51:9227–9234.